RSC Advances

PAPER

View Article Online
View Journal | View Issue

Open Access Article. Published on 29 September 2025. Downloaded on 4/1/2026 5:04:42 PM.
This article is licensed under a Creative Commons Attribution-NonCommercial 3.0 Unported Licence.

Check for updates

Cite this: *RSC Adv.*, 2025, **15**, 35921

Co-allosteric hairpin probe for detecting microRNA with high specificity

Tingting Cao,[ab] Yi Wang[ab] and Xiaolin Yu*[ab]

Received 24th July 2025
Accepted 25th September 2025

DOI: 10.1039/d5ra05363c

rsc.li/rsc-advances

MicroRNAs have emerged as crucial biomarkers for disease diagnosis and prognosis, while their accurate detection remains challenging due to high sequence homology among family members. In this study, a co-allosteric hairpin (CA-HP) probe was designed for highly specific microRNA detection. The CA-HP probe leverages synergistic interactions between the target miRNA and a helper strand to induce a conformational change, resulting in fluorescence activation only upon perfectly matched target recognition. By optimizing the complementary lengths of the target and helper strands, the system achieves significantly enhanced specificity compared to conventional hairpin probes. This strategy offers a robust and facile approach for accurate miRNA profiling, which is crucial for clinical diagnostics and personalized medicine. The CA-HP design also provides a generalizable framework for developing high-specificity nucleic acid probes.

1. Introduction

MicroRNAs (miRNAs) are a group of small, non-coding RNA molecules that range from approximately 18 to 24 nucleotides in length and play crucial roles in various physiological processes such as cell differentiation, apoptosis, and growth.[1–4] With the application of high-throughput sequencing technology, a large number of studies have shown that aberrant expression of miRNAs is closely associated with tumor development and progression. miRNAs are considered promising molecules for cancer recognition, opening new avenues for the diagnosis and treatment of malignant diseases, including liver and lung cancer.[5–7] Differences in miRNA expression profiles in normal, adjacent and tumor tissues help to reveal the molecular mechanisms of tumor development.[8–10] By detecting miRNAs non-invasively, physicians can implement effective gene therapy and assess disease risk at an early stage. Therefore, the development of rapid, sensitive and quantitative circulating miRNA detection platforms and technologies has attracted considerable attention.

Some significant advancements have been achieved in the enhancement of sensitivity, a critical performance metric. This progress is largely attributed to the utilization of quantum dots,[11–13] nanoparticles,[14–16] amplification methodologies,[17–19] and other technologies. The specificity of the detection method is also important in the study of miRNAs because of their high sequence homology, which is closely related to the nature of diseases, medication and prognosis.[20–25] Droplet digital PCR (ddPCR) directly increases the sensitivity of the assay and improves the purity to a certain extent, thus increasing the specificity.[26] Chen *et al.* demonstrated a new method based on the rational design and optimization of closed symmetric dumbbell nucleic acid amplification templates, which takes into account the free energies of various target molecules to design compact rigid templates with standard free energy.[27] Only the target miRNAs trigger the thermostatic exponential amplification reaction and effectively suppress non-specific hybridization amplification. Johnson-Buck *et al.* determined the correct bases among the four bases by multiple calculations of the Poisson distribution.[28] Krzywkowski and Nilsson systematically investigated the optimal conditions for RNA probe binding and detection.[29] The specific recognition of ligases is used to improve the specificity of miRNA detection. However, this method usually requires elaborate designs or unstable enzymes.

Hairpin DNA is a type of single-stranded DNA capable of folding into a stem-and-loop structure characterized by a complementary duplex double-stranded region and an unpaired loop portion.[30–32] A free nucleic acid fragment, often referred to as the toehold region, usually extends from the complementary duplex double-stranded region. The target is complementary to the toehold domain of the hairpin and the stem to which it is attached, and the double strand of the hairpin is opened by a toehold-mediated strand displacement reaction. The hairpin changes from a partially double-stranded to a single-stranded structure. The conformational change results in a change in fluorescence or the release of bases that trigger subsequent reactions.

In this study, the helper chain was introduced to play the role of co-opening the hairpin with the target. The ends of the

[a]*Department of Laboratory Medicine, Sichuan Clinical Research Center for Clinical Laboratory, Zigong Fourth People's Hospital, Sichuan, 643000, China. E-mail: yuxiaolincq@hotmail.com; Fax: +86-813-7424885; Tel: +86-813-7424885*

[b]*Institute of Precision Medicine, Zigong Academy of Big Data and Artificial Intelligence in Medical Science, Sichuan, 643000, China*

© 2025 The Author(s). Published by the Royal Society of Chemistry

Open Access Article. Published on 29 September 2025. Downloaded on 4/1/2026 5:04:42 PM.
This article is licensed under a Creative Commons Attribution-NonCommercial 3.0 Unported Licence.

hairpin are modified with fluorescent and quenching clusters, and the opening and closing of the fluorescent signal occurs when the hairpin changes conformation. The lengths of the target and helper chains can be varied to change the weights they play in opening the hairpin. In conventional hairpin probes, the target is overwhelmed and the hairpin is also switched on when there are mismatched bases in the target DNA. The co-allosteric hairpin (CA-HP) probe designed in this study is designed to achieve a state where both the target and the helper are indispensable. The helper does not cooperate with the mismatched target and the hairpin probe is not opened. This multi-strand verification mechanism significantly enhances specificity. It helps to identify miRNA accurately so that it can be used correctly and rationally to treat the disease.

2. Experimental

2.1. Materials and reagents

2.1.1. Oligonucleotide synthesis. DNA and RNA oligonucleotides used in this study were purchased from Sangon Biotech Co. (Shanghai, China). Lba Cas12a (Cpf1, 20 μM) and rCutSmart buffer were bought from New England Biolabs (Beijing, China). All used DNA and RNA sequences are listed in Table S1. All DNA oligonucleotides were purified *via* high-performance liquid chromatography (HPLC). The hairpin probes were modified with FAM and quenched strands with BHQ1.

2.1.2. Buffer conditions. All DNA oligonucleotides were redissolved in TE buffer, consisting of Tris-HCl (10 mM) and EDTA (1 mM). The buffer used in the annealing step and fluorescence experiment was TE buffer with $MgCl_2$ (12.5 mM).

2.2. Fluorescence experiment

Hairpin probes were dissolved to 10 μM in the TE buffer. The solution was diluted to 2 μM in TEMg and then annealed in a polymerase chain reaction (PCR) thermal cycler. The temperature was set at 95 °C for 5 min and cooled down to 20 °C by 0.1 °C s^{-1}. All time-based fluorescence data were acquired using a Real-Time PCR Detection System. The temperature was set to 37 °C. All fluorescent signals were monitored under the green channel. Signal-to-noise ratio = $(S_{target} - S_0)/(S_{no\ target} - S_0)$. DF = $(S_{pM} - S_{background})/(S_{Mis} - S_{background})$. S_0 is the initial signal. S_{pM} is a signal of perfectly matched target, $S_{background}$ is a signal without target, and S_{Mis} is a signal of mismatched target. The fluorescence intensities presented in Figures are values taken from the fluorimeter.

3. Results and discussion

3.1. Co-allosteric hairpin probe with helper

As shown in Fig. 1A, the 5′-end of the hairpin is modified with a green fluorophore and the 3′-end is modified with a quenching group. When the hairpin is folded, the fluorophore and the quenching group are spatially close to each other and the fluorescence signal is quenched. The target is defined as input (I) and the helper chain is abbreviated as H. I is complementary to the 3-terminal stem and H is complementary to the 5-terminal stem. However, the complementary forces are smaller than the intra-strand hybridization forces of the hairpin. Only when both I and H are present can they act on the hairpin. If only I or H is present (Fig. 1B), a temporarily opened hairpin will displace either I or H and will not produce a fluorescent signal.

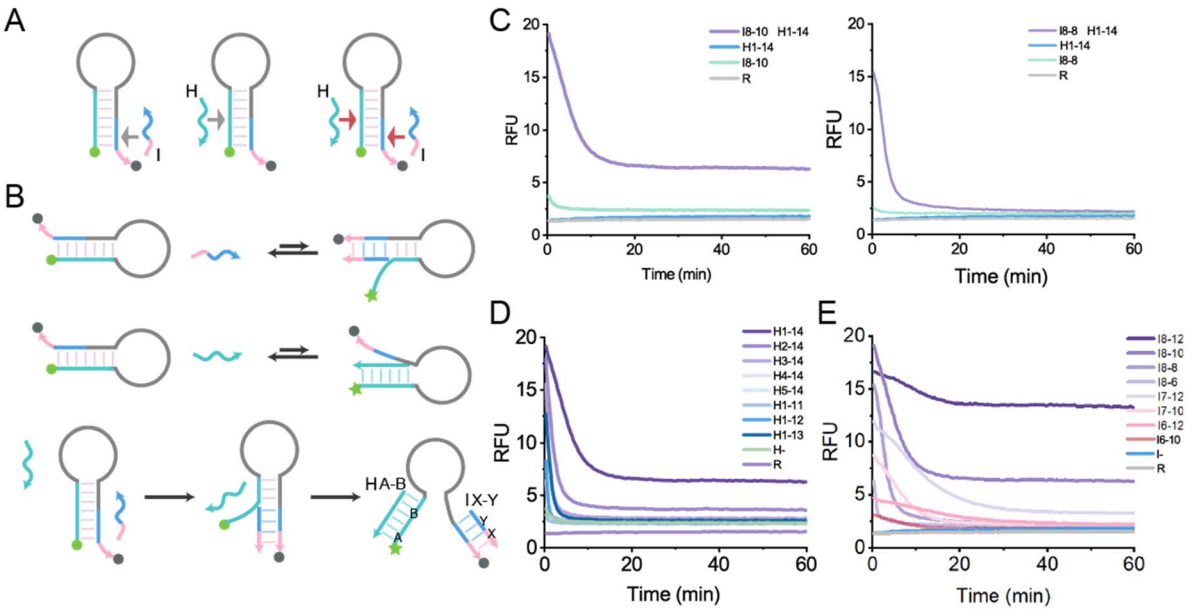

Fig. 1 Co-allosteric hairpin probe with helper. All experiments were performed at 37 °C in TEMg buffer. (A) Collaboration of I and H. (B) Schematic diagram of the collaboration between I and H. (C) Fluorescence curves of collaboration between I and H. (D) I8-10 collaborate with different lengths of H. (E) H1-14 collaborate with different I. + means that a strand exists, − means that a strand does not exist. X in IX-Y represents toehold length and Y represents branch migration length. HA-B means H is complementary with the Ath base to the Bth base from the 5′ of the hairpin. R stands for hairpin probe. The concentrations of H, I and R are 200 nM.

 © 2025 The Author(s). Published by the Royal Society of Chemistry

Open Access Article. Published on 29 September 2025. Downloaded on 4/1/2026 5:04:42 PM.
This article is licensed under a Creative Commons Attribution-NonCommercial 3.0 Unported Licence.

Only when I is present does the stem become partially opened by toehold-mediated chain displacement reaction. The opened stem acts as a new toehold bound by H and extends further. When the hairpin was fully opened, a fluorescent signal was generated. The fluorescence experiments showed that the initial fluorescence signal was significantly higher when I was present together with H than when it was present alone (Fig. 1C and S1–S17). However, the fluorescence gradually decreased over time. This may be due to the fact that the loop region becomes flexible single-stranded nucleic acid after the hairpin is opened, which shortens the distance between fluorescence and quenching. As I shortened, the rigid double-stranded length shortened, the single-stranded nucleic acid region becomes longer and the fluorescence value decreased more (Fig. 1C and S1–S17). Different H lengths have different cooperative effects with I (Fig. 1D). The longer H leads to the higher initial and terminal fluorescence. Changing cooperative effects were also observed when H was fixed and the toehold and branch migration lengths of I varied (Fig. 1E).

3.2. Co-allosteric hairpin probe with CL

Considering the effect of the loop on the fluorescence signal after the hairpin is fully opened, a nucleic acid complementary to the loop (CL) was designed (Fig. 2A). CL cooperates with H and I to open the hairpin probe. The rigid double-stranded region between the fluorescence and the quenching motif becomes longer and the fluorescence is less likely to be quenched. The lengths and binding regions of H and CL were optimized empirically based on the free energy of hybridization and the stability of the stem-loop structure. We systematically varied hybridization length of H and CL. The fluorescence signals generated by different CLs interacting with I8-10 and H1-14 are shown in Fig. 2B. The fluorescence signals gradually increased with increasing CL length, forming a clear difference from the fluorescence signals in the absence of I (blue bars). This illustrated the effectiveness of the cooperation of CL with I (Fig. S18–S23). The concentration of I and the hairpin probe was fixed at 200 nM, which are cooperated with different concentrations of H and L (Fig. 2C). As the concentration increased, the ratio of positive signal to background signal gradually decreased. Therefore, 200 nM was chosen as the optimal concentration. The results of I8-8 cooperated with different H and different CL also proved the successful cooperation of CL (Fig. 2D).

3.3. Co-allosteric hairpin probe with high specificity of I

Mismatched bases are introduced at different positions of I. The identification factor (DF) of traditional hairpin probes needs to be improved. DF at most mutation sites was less than 5, only 7.3 when mismatch was in the middle (Fig. S24). The identification of mutations at both ends was the worst, with DF less than 2. The specificity of different combinations of Co-allosteric hairpin probes was tested. When different mutations were introduced in I8-8, DF reached a maximum of 85 (Fig. 3A and S25). When H1-14 CL14, the DF of M1 is 24. However, the DF of the M6 is still less than ideal, being less than 2. When different mutations were introduced in I8-9, DF reached a maximum of 63 (Fig. 3B). When H1-14 CL13, the DF of M1 is 15.6. However,

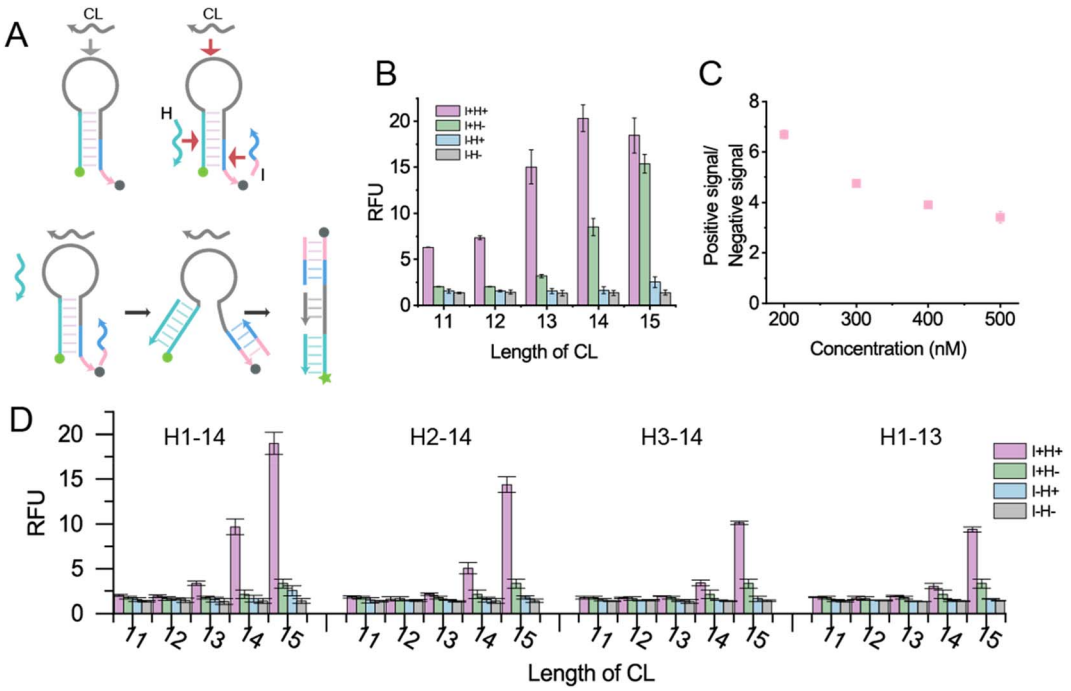

Fig. 2 Co-allosteric hairpin probe with CL. All experiments were performed at 37 °C in TEMg buffer. (A) CL cooperation diagram. (B) I8-10 and H1-14 cooperated with different lengths of CL. (C) Optimization of H and CL concentration. The concentration of I and R was fixed at 200 nM. The concentrations of H and CL are the same. (D) Fluorescence results of I8-8 cooperating with different H and different CL. Except for (C), the concentrations of H, I, CL and R are 200 nM. Error bars represent ± standard deviation (SD) from three independent experiments ($n = 3$).

Open Access Article. Published on 29 September 2025. Downloaded on 4/1/2026 5:04:42 PM.
This article is licensed under a Creative Commons Attribution-NonCommercial 3.0 Unported Licence.

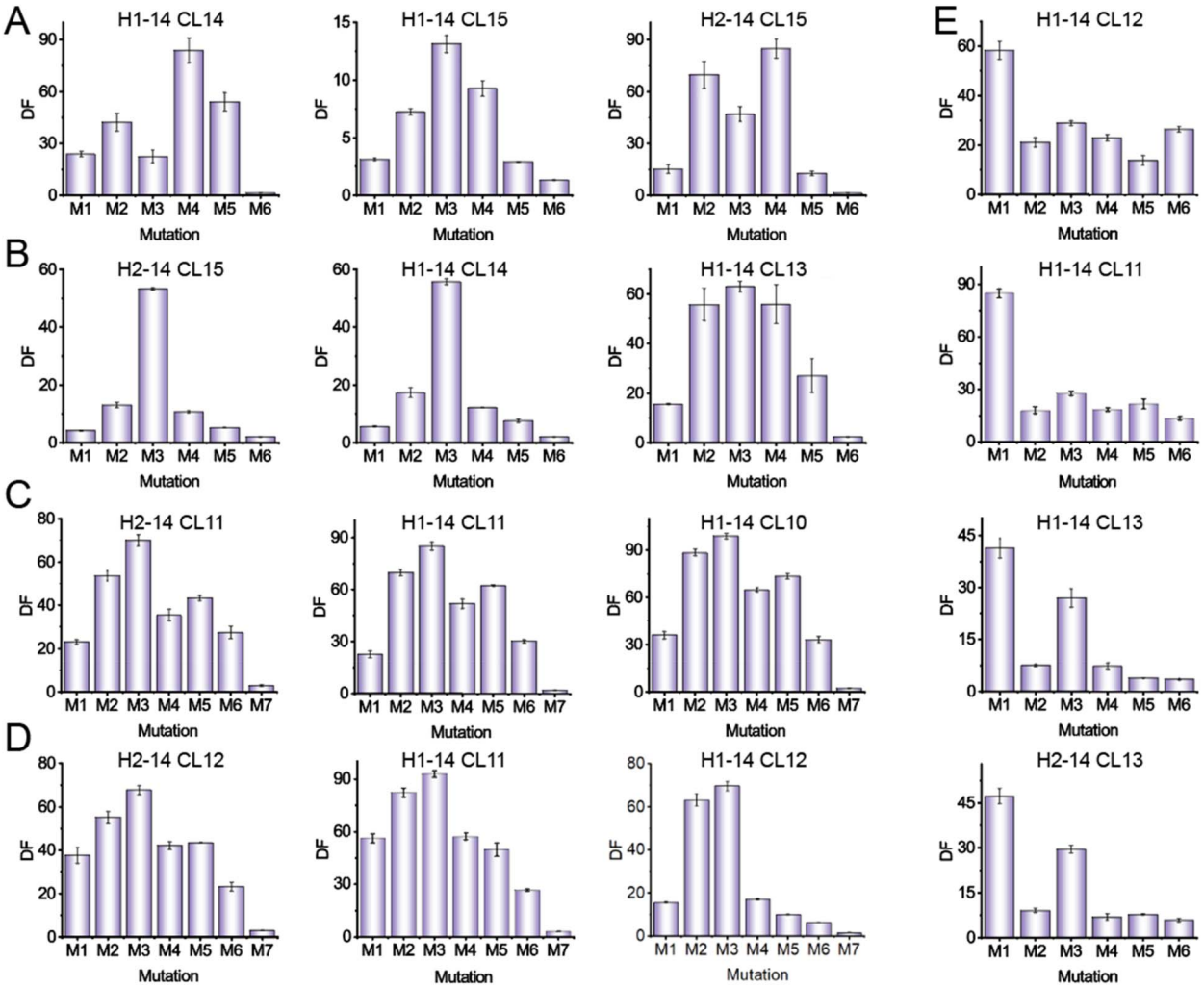

Fig. 3 Co-allosteric hairpin probe with high specificity of I. All experiments were performed at 37 °C in TEMg buffer. The DF of I8-8 (A), I8-9 (B), I8-10 (E), I8-11 (C) and I8-12 (D) with different mutations. The concentrations of H, I, CL and R are 200 nM. Error bars represent ± standard deviation (SD) from three independent experiments ($n = 3$).

the DF of M6 is still less than ideal, at 2.3 when H1-14 CL13. When different mutations were introduced in I8-10, DF reached a maximum of 85 (Fig. 3E). It is worth mentioning that when H1-14 CL11, the DF of M1 is 85. At H1-14 CL12, the DF of M6 is 26.5. When different mutations were introduced in I8-11, DF reached a maximum of 99 (Fig. 3C). At H1-14CL10, the DF of M1 is 36.0. However, the DF of M6 is not ideal, at 2.9 when H2-14CL11. When different mutations were introduced in I8-12, DF reached a maximum of 93 (Fig. 3D). At H1-14CL11, the DF of M1 is 56.3. Similarly, the DF of M6 is still not ideal, at 3.2 when H1-14CL11. It can be seen that the specificity of CA-HP is better than that of traditional hairpin probe. Improved specificity was also achieved when shortening the toehold length of I and validating against end-base mismatches (Fig. S26 and S27).

3.4. Co-allosteric hairpin probe with high specificity of CL

Inspired by the importance of CL in hairpin probes, CL was reversed as a target for experiments. Mismatched bases were introduced at different locations of CL. According to the fluorescence results in Fig. 4, different H and CL were matched for different types of I. When I with 7 nt toehold as helper to open the hairpin probe, DF was up to 181. The maximum DF of the M1 and M10 was 30.0 and 18.5 (Fig. 4A and S28). When I with toehold of 8 nt is used as a helper to open the hairpin probe, DF was up to 191. The DF of M1 and M6 can be up to 39.2 and 21.3 (Fig. 4B). This demonstrated the high specificity of CL recognition. The end-identification effects of traditional hairpin probes, which is I as a target, and CL as a target were synthesized (Fig. 4C). The identification effect of the terminal mutation was enhanced in CL, superior to that of the mutation in I. CL13 showed the best results.

3.5. Co-allosteric hairpin probe for micro-122 detection

MicroRNA-122 (micro-122) has significant value in the diagnosis, monitoring and prognosis of liver disease. Changes in its levels can reflect the degree of liver damage and aid in early diagnosis and evaluation of therapeutic efficacy, making it an important biomarker in the study and treatment of liver

 © 2025 The Author(s). Published by the Royal Society of Chemistry

Open Access Article. Published on 29 September 2025. Downloaded on 4/1/2026 5:04:42 PM.
This article is licensed under a Creative Commons Attribution-NonCommercial 3.0 Unported Licence.

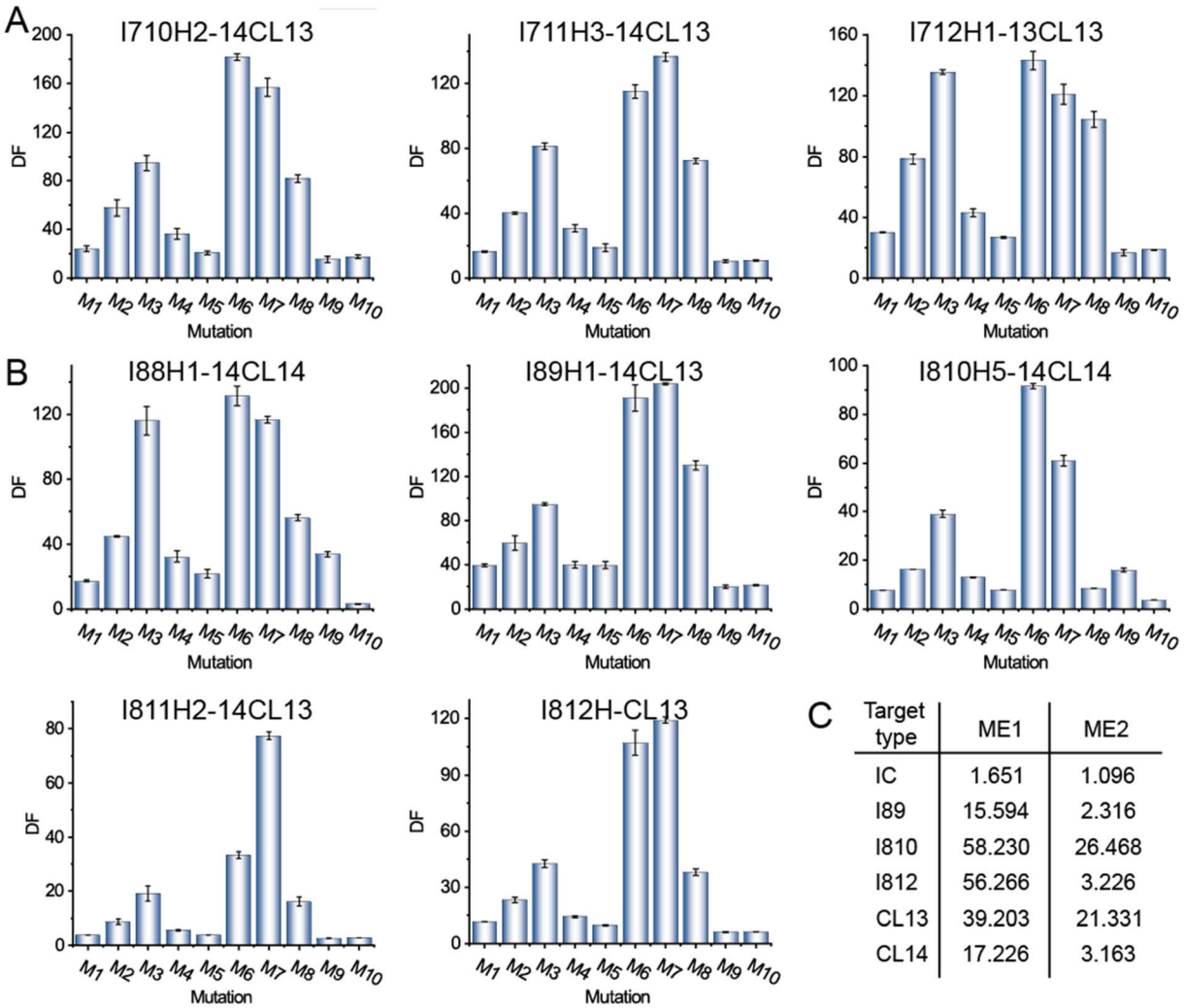

Target type	ME1	ME2
IC	1.651	1.096
I89	15.594	2.316
I810	58.230	26.468
I812	56.266	3.226
CL13	39.203	21.331
CL14	17.226	3.163

Fig. 4 Co-allosteric hairpin probe with high specificity of CL. All experiments were performed at 37 °C in TEMg buffer. (A) CL specificity of I with 7 nt toehold. (B) CL specificity of I with 8 nt toehold. (C) Summary of identification effect of different types of targets. IC stands for traditional hairpin probe. The concentrations of H, I, CL and R are 200 nM. Error bars represent ± standard deviation (SD) from three independent experiments (n = 3).

disease.[33,34] Changes in its levels can reflect the degree of liver damage and aid in early diagnosis and evaluation of therapeutic efficacy, making it an important biomarker in the study and treatment of liver disease.[33,34] Using micro-122 as a target, the sequence of micro-122 is set in CL region and the hairpin probe was opened cooperatively with H and I (Fig. 5A). Fluorescence experiments showed a clear difference between positive and negative signals and different H, I had different effects (Fig. 5A). Different mismatches were set in micro-122. In the case of I8-16 with H3-24 (Fig. 5B and S29) or I8-18 with H3-24 (Fig. 5C), CA-HP showed a satisfactory ability to identify mutations. Gel electrophoresis also validated the feasibility of CA-HP (Fig. S30). Furthermore, a linear correlation between fluorescence intensity and target concentration was observed in the range 0.1–20 nM. The corresponding equation is $F = 10.322 + 4.218 \lg x (R^2 = 0.99)$, and the detection limit is calculated as 0.13 nM using the $3\sigma/S$ rule (Fig. 5D). GC content of sequence has a great influence on the signal leakage. The effect of GC content in toehold and stem domain on the reaction was tested (Fig. S31). When the GC content of toehold and stem domain is too high, the leakage is obvious. The effect of GC content on the positive signal in stem domain is negligible. The positive signal decreased when GC content of toehold was too low. This may be attributed to the hybridization of toehold drives strand displacement reactions. The stem of hairpin is complementary within the strand. In addition, the loop of CA-HP was modified to detect micro-122 and let-7a (Fig. S32). The results showed that all DF of different sites were >10, which proved that the method could be extended to other miRNAs. Combined with other isothermal amplification strategies, it is expected to achieve highly sensitive and highly specific microRNA detection. We combined CA-HP with autocatalytic CRISPR system. The microRNA-122 of 1 fM can also be distinguished from the background signal, and its sensitivity is superior to that of CA-HP alone (Fig. S33). The specificity of the system is also satisfactory. The signals generated by non-target microRNAs are

Open Access Article. Published on 29 September 2025. Downloaded on 4/1/2026 5:04:42 PM.
This article is licensed under a Creative Commons Attribution-NonCommercial 3.0 Unported Licence.

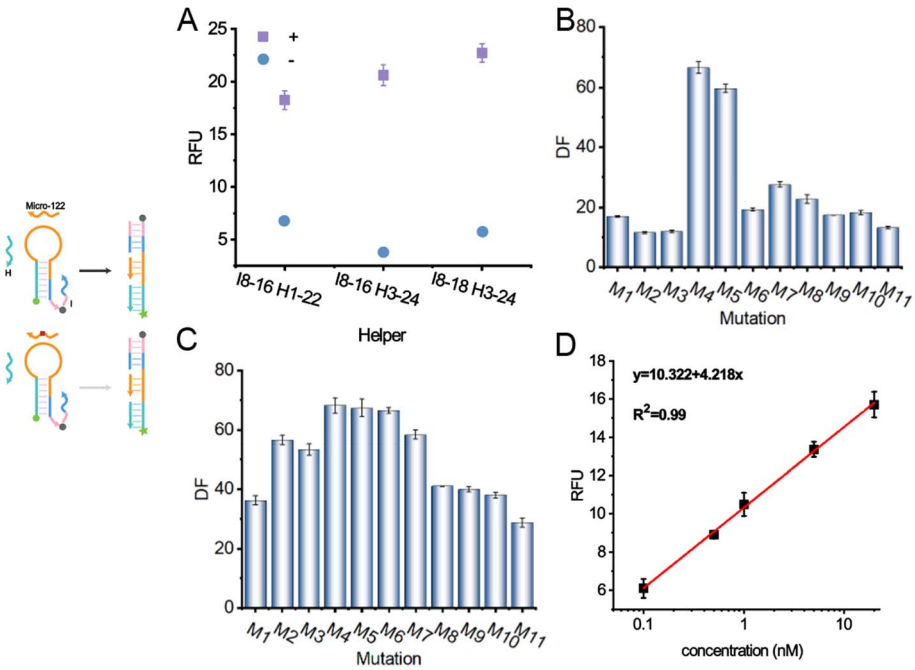

Fig. 5 Co-allosteric hairpin probe for micro-122 detection. (A) Different I and H fluorescence signals. DF of I8-16 with H3-24 (B) or I8-18 with H3-24 (C). (D) Linear relationship between fluorescence intensity and target concentration. All experiments were performed at 37 °C in TEMg buffer. Except for (D), the concentrations of H, I, micro-122 and R are 200 nM. Error bars represent ± standard deviation (SD) from three independent experiments ($n = 3$).

similar to the background signal. All these demonstrated the potential of CA-HP to be applied in clinical detection. To assess the capability of this analytical method in detecting real samples, serum samples (healthy people) were collected. Micro-122 of different concentrations was added to 10 times diluted serum. The recovery test results, as shown in Table S2, the method exhibited recovery rates ranging from 100.8% to 107.7% (RSD = 2.3–9.2%). Therefore, this method also shows good application potential in the analysis of complex clinical matrix. A comparison with other miRNA detection methods demonstrated that CA-HP is a simple, highly specific, and modularizable strategy (Table S3). However, challenges such as interference from homologous DNA, pri-microRNA, and protein-bound microRNAs in serum should be considered. Further optimization may be required for whole blood samples.

4. Conclusion

miRNAs, with their exceptional tissue stability, have emerged as a highly promising disease biomarker.[35–37] Especially in the diagnosis and research of liver and lung cancers, the abnormal expression patterns of miRNAs have unveiled molecular mechanisms underlying tumorigenesis, providing invaluable clues.[38,39] However, the issue of specificity in miRNAs detection has always been a focus of attention due to the high similarity among homologous miRNAs, which has limited the depth and breadth of its clinical applications to some extent. In response to this challenge, we propose the CA-HP strategy, namely the collaborative hairpin probe technology, aimed at significantly enhancing the specificity of miRNAs detection. The advantage of this strategy is that the specificity of micro-122 detection can be easily improved through the helper strand. Only when both the helper and target function synergistically can the CA-HP output a fluorescent signal. Conformational changes are triggered through synergistic effect.[40] In addition, it is easy to combine with other isothermal amplification strategies to achieve highly sensitive and highly specific detection. Through ingenious molecular design, CA-HP can achieve precise recognition of target miRNAs and effectively distinguish homologous miRNAs, thereby solving the long-standing specificity problem that has plagued researchers. However, detecting non-nucleic acid targets remains challenging and may require combination with strategies such as aptamer.

We believe that the CA-HP strategy also holds tremendous potential for applications in single nucleotide polymorphism (SNP) detection and intracellular imaging because of its good biocompatibility. However, it is necessary to overcome the problem that it is easily degraded by biological enzymes. Combining with chemical modification could enhance enzymatic stability for *in vivo* applications. In the field of SNP detection, the high specificity of CA-HP will enable us to more accurately identify SNP sites associated with diseases, providing powerful support for early disease warning and precision treatment. Furthermore, with further optimization and improvement, CA-HP is expected to become an efficient SNP genotyping tool, driving in-depth developments in genomics research. In the field of intracellular imaging, the CA-HP strategy also demonstrates broad application prospects. It can be utilized to achieve real-time, dynamic monitoring of specific

 © 2025 The Author(s). Published by the Royal Society of Chemistry

Open Access Article. Published on 29 September 2025. Downloaded on 4/1/2026 5:04:42 PM.
This article is licensed under a Creative Commons Attribution-NonCommercial 3.0 Unported Licence.

miRNA molecules, providing intuitive and powerful evidence for revealing intracellular and extracellular signal transduction mechanisms and exploring molecular events during the onset and progression of diseases.[41–45] It is expected to provide new technical means for drug screening, efficacy assessment, and other purposes, promoting continuous advancements in biomedical research.[46–50]

In summary, the CA-HP strategy not only provides new ideas and solutions for miRNA detection but also demonstrates enormous potential for applications in SNP detection and intracellular imaging, expanding the tools available for biomedical research and clinical diagnosis and treatment.

Abbreviation

CA-HP	co-allosteric hairpin
miRNAs	microRNAs
ddPCR	droplet digital PCR
SNP	single nucleotide polymorphism

Author contributions

Tingting Cao: writing – original draft, methodology, investigation, formal analysis, data curation. Yi Wang: methodology, investigation, formal analysis, data curation. Xiaolin Yu: writing – review & editing, validation, resources, methodology, investigation, funding acquisition, conceptualization.

Conflicts of interest

The authors declare that there is no conflict of interest regarding the publication of this article.

Data availability

The data are available from the corresponding author upon reasonable request.

Supplementary information: Fig. S1–S33 and Table S1–S3. See DOI: https://doi.org/10.1039/d5ra05363c.

Acknowledgements

This work was funded by the financial support from the Natural Science Foundation General Program of Sichuan (2022NSFSC0810), the Key Science and Technology Project of Zigong (2022ZCYGY02).

References

1 T. Fehlmann, M. Kahraman, N. Ludwig, C. Backes, V. Galata, V. Keller, L. Geffers, N. Mercaldo, D. Hornung, T. Weis, E. Kayvanpour, M. Abu-Halima, C. Deuschle, C. Schulte, U. Suenkel, A. K. von Thaler, W. Maetzler, C. Herr, S. Fähndrich, C. Vogelmeier, P. Guimaraes, A. Hecksteden, T. Meyer, F. Metzger, C. Diener, S. Deutscher, H. Abdul-Khaliq, I. Stehle, S. Haeusler, A. Meiser, H. V. Groesdonk, T. Volk, H. P. Lenhof, H. Katus, R. Balling, B. Meder, R. Kruger, H. Huwer, R. Bals, E. Meese and A. Keller, Evaluating the Use of Circulating MicroRNA Profiles for Lung Cancer Detection in Symptomatic Patients, *JAMA Oncol.*, 2020, **6**, 714–723.

2 L. J. Galvão-Lima, A. H. F. Morais, R. A. M. Valentim and E. Barreto, miRNAs as biomarkers for early cancer detection and their application in the development of new diagnostic tools, *Biomed. Eng. Online*, 2021, **20**, 21.

3 L. Valihrach, P. Androvic and M. Kubista, Circulating miRNA analysis for cancer diagnostics and therapy, *Mol. Aspects Med.*, 2020, **72**, 100825.

4 W. Usuba, F. Urabe, Y. Yamamoto, J. Matsuzaki, H. Sasaki, M. Ichikawa, S. Takizawa, Y. Aoki, S. Niida, K. Kato, S. Egawa, T. Chikaraishi, H. Fujimoto and T. Ochiya, Circulating miRNA panels for specific and early detection in bladder cancer, *Cancer Sci.*, 2019, **110**, 408–419.

5 M. A. Iqbal, S. Arora, G. Prakasam, G. A. Calin and M. A. Syed, MicroRNA in lung cancer: role, mechanisms, pathways and therapeutic relevance, *Mol. Aspects Med.*, 2019, **70**, 3–20.

6 N. Asano, J. Matsuzaki, M. Ichikawa, J. Kawauchi, S. Takizawa, Y. Aoki, H. Sakamoto, A. Yoshida, E. Kobayashi, Y. Tanzawa, R. Nakayama, H. Morioka, M. Matsumoto, M. Nakamura, T. Kondo, K. Kato, N. Tsuchiya, A. Kawai and T. Ochiya, A serum microRNA classifier for the diagnosis of sarcomas of various histological subtypes, *Nat. Commun.*, 2019, **10**, 1299.

7 E. Callegari, L. Gramantieri, M. Domenicali, L. D'Abundo, S. Sabbioni and M. Negrini, MicroRNAs in liver cancer: a model for investigating pathogenesis and novel therapeutic approaches, *Cell Death Differ.*, 2015, **22**, 46–57.

8 M. Herreros-Villanueva, S. Duran-Sanchon, A. C. Martín, R. Pérez-Palacios, E. Vila-Navarro, M. Marcuello, M. Diaz-Centeno, J. Cubiella, M. S. Diez, L. Bujanda, A. Lanas, R. Jover, V. Hernández, E. Quintero, J. José Lozano, M. García-Cougil, I. Martínez-Arranz, A. Castells, M. Gironella and R. Arroyo, Plasma MicroRNA Signature Validation for Early Detection of Colorectal Cancer, *Clin. Transl. Gastroenterol.*, 2019, **10**, e00003.

9 S. Cai, T. Pataillot-Meakin, A. Shibakawa, R. Ren, C. L. Bevan, S. Ladame, A. P. Ivanov and J. B. Edel, Single-molecule amplification-free multiplexed detection of circulating microRNA cancer biomarkers from serum, *Nat. Commun.*, 2021, **12**, 3515.

10 L. Ng, R. W. Sin, D. H. Cheung, C. K. Wong, C. L. Lam, W. K. Leung, W. L. Law and D. C. Foo, Identification and evaluation of a serum microRNA panel to diagnose colorectal cancer patients, *Int. J. Cancer*, 2024, **156**, 865–874.

11 J. Ge, Y. Hu, R. Deng, Z. Li, K. Zhang, M. Shi, D. Yang, R. Cai and W. Tan, Highly Sensitive MicroRNA Detection by Coupling Nicking-Enhanced Rolling Circle Amplification with MoS(2) Quantum Dots, *Anal. Chem.*, 2020, **92**, 13588–13594.

12 C. S. M. Martins, A. P. LaGrow and J. A. V. Prior, Quantum Dots for Cancer-Related miRNA Monitoring, *ACS Sens.*, 2022, **7**, 1269–1299.

Open Access Article. Published on 29 September 2025. Downloaded on 4/1/2026 5:04:42 PM.
This article is licensed under a Creative Commons Attribution-NonCommercial 3.0 Unported Licence.

13 W. J. Liu, L. J. Wang and C. Y. Zhang, Progress in quantum dot-based biosensors for microRNA assay: A review, *Anal. Chim. Acta*, 2023, **1278**, 341615.
14 I. Gessner, J. W. U. Fries, V. Brune and S. Mathur, Magnetic nanoparticle-based amplification of microRNA detection in body fluids for early disease diagnosis, *J. Mater. Chem. B*, 2021, **9**, 9–22.
15 K. Yang, J. Li, M. Lamy de la Chapelle, G. Huang, Y. Wang, J. Zhang, D. Xu, J. Yao, X. Yang and W. Fu, A terahertz metamaterial biosensor for sensitive detection of microRNAs based on gold-nanoparticles and strand displacement amplification, *Biosens. Bioelectron.*, 2021, **175**, 112874.
16 T. Lee, M. Mohammadniaei, H. Zhang, J. Yoon, H. K. Choi, S. Guo, P. Guo and J. W. Choi, Single Functionalized pRNA/Gold Nanoparticle for Ultrasensitive MicroRNA Detection Using Electrochemical Surface-Enhanced Raman Spectroscopy, *Adv. Sci.*, 2020, **7**, 1902477.
17 Y. Yang, J. Yang, F. Gong, P. Zuo, Z. Tan, J. Li, C. Xie, X. Ji, W. Li, Z. J. S. He and A. B. Chemical, Combining CRISPR/Cas12a with isothermal exponential amplification as an ultrasensitive sensing platform for microRNA detection, *Sens. Actuators, B*, 2022, **367**, 132158.
18 G. Gines, R. Menezes, K. Nara, A. S. Kirstetter, V. Taly and Y. Rondelez, Isothermal digital detection of microRNAs using background-free molecular circuit, *Sci. Adv.*, 2020, **6**, eaay5952.
19 D. Li, T. Zhang, F. Yang, R. Yuan and Y. Xiang, Efficient and Exponential Rolling Circle Amplification Molecular Network Leads to Ultrasensitive and Label-Free Detection of MicroRNA, *Anal. Chem.*, 2020, **92**, 2074–2079.
20 T. Ouyang, Z. Liu, Z. Han and Q. Ge, MicroRNA Detection Specificity: Recent Advances and Future Perspective, *Anal. Chem.*, 2019, **91**, 3179–3186.
21 J. Ye, M. Xu, X. Tian, S. Cai and S. Zeng, Research advances in the detection of miRNA, *J. Pharm. Anal.*, 2019, **9**, 217–226.
22 S. Shin, Y. Jung, H. Uhm, M. Song, S. Son, J. Goo, C. Jeong, J. J. Song, V. N. Kim and S. Hohng, Quantification of purified endogenous miRNAs with high sensitivity and specificity, *Nat. Commun.*, 2020, **11**, 6033.
23 A. Miti, S. Thamm, P. Müller, A. Csáki, W. Fritzsche and G. Zuccheri, A miRNA biosensor based on localized surface plasmon resonance enhanced by surface-bound hybridization chain reaction, *Biosens. Bioelectron.*, 2020, **167**, 112465.
24 H. Yan, Y. Wen, Z. Tian, N. Hart, S. Han, S. J. Hughes and Y. Zeng, A one-pot isothermal Cas12-based assay for the sensitive detection of microRNAs, *Nat. Biomed. Eng.*, 2023, **7**, 1583–1601.
25 T. D. Canady, N. Li, L. D. Smith, Y. Lu, M. Kohli, A. M. Smith and B. T. Cunningham, Digital-resolution detection of microRNA with single-base selectivity by photonic resonator absorption microscopy, *Proc. Natl. Acad. Sci. U. S. A.*, 2019, **116**, 19362–19367.
26 H. Tian, Y. Sun, C. Liu, X. Duan, W. Tang and Z. Li, Precise Quantitation of MicroRNA in a Single Cell with Droplet Digital PCR Based on Ligation Reaction, *Anal. Chem.*, 2016, **88**, 11384–11389.
27 J. Chen, T. An, Y. Ma, B. Situ, D. Chen, Y. Xu, L. Zhang, Z. Dai and X. Zou, Isothermal Amplification on a Structure-Switchable Symmetric Toehold Dumbbell-Template: A Strategy Enabling MicroRNA Analysis at the Single-Cell Level with Ultrahigh Specificity and Accuracy, *Anal. Chem.*, 2018, **90**, 859–865.
28 A. Johnson-Buck, X. Su, M. D. Giraldez, M. Zhao, M. Tewari and N. G. Walter, Kinetic fingerprinting to identify and count single nucleic acids, *Nat. Biotechnol.*, 2015, **33**, 730–732.
29 T. Krzywkowski and M. Nilsson, Fidelity of RNA templated end-joining by chlorella virus DNA ligase and a novel iLock assay with improved direct RNA detection accuracy, *Nucleic Acids Res.*, 2017, **45**, e161.
30 R. Abolhasan, A. Mehdizadeh, M. R. Rashidi, L. Aghebati-Maleki and M. Yousefi, Application of hairpin DNA-based biosensors with various signal amplification strategies in clinical diagnosis, *Biosens. Bioelectron.*, 2019, **129**, 164–174.
31 F. Li, W. Yu, J. Zhang, Y. Dong, X. Ding, X. Ruan, Z. Gu and D. Yang, Spatiotemporally programmable cascade hybridization of hairpin DNA in polymeric nanoframework for precise siRNA delivery, *Nat. Commun.*, 2021, **12**, 1138.
32 M. Rossetti, R. Merlo, N. Bagheri, D. Moscone, A. Valenti, A. Saha, P. R. Arantes, R. Ippodrino, F. Ricci, I. Treglia, E. Delibato, J. van der Oost, G. Palermo, G. Perugino and A. Porchetta, Enhancement of CRISPR/Cas12a trans-cleavage activity using hairpin DNA reporters, *Nucleic Acids Res.*, 2022, **50**, 8377–8391.
33 A. A. Mohamed, D. M. Abo-Elmatty, O. Ezzat, N. M. Mesbah, N. S. Ali, A. S. Abd El Fatah, E. Alsayed, M. Hamada, A. A. Hassnine, S. Abd-Elsalam, A. Abdelghani, M. B. Hassan and S. A. Fattah, Pro-Neurotensin as a Potential Novel Diagnostic Biomarker for Detection of Nonalcoholic Fatty Liver Disease, *Diabetes, Metab. Syndr. Obes.*, 2022, **15**, 1935–1943.
34 B. Cheng, Q. Zhu, W. Lin and L. Wang, MicroRNA-122 inhibits epithelial-mesenchymal transition of hepatic stellate cells induced by the TGF-β1/Smad signaling pathway, *Exp. Ther. Med.*, 2019, **17**, 284–290.
35 Y. Zhou, Q. Li, R. Pan, Q. Wang, X. Zhu, C. Yuan, F. Cai, Y. D. Gao and Y. Cui, Regulatory roles of three miRNAs on allergen mRNA expression in Tyrophagus putrescentiae, *Allergy*, 2022, **77**, 469–482.
36 Q. Zhu, J. Sun, C. An, X. Li, S. Xu, Y. He, X. Zhang, L. Liu, K. Hu and M. Liang, Mechanism of LncRNA Gm2044 in germ cell development, *Front. Cell Dev. Biol.*, 2024, **12**, 1410914.
37 M. H. Bao, G. Y. Li, X. S. Huang, L. Tang, L. P. Dong and J. M. Li, Long Noncoding RNA LINC00657 Acting as a miR-590-3p Sponge to Facilitate Low Concentration Oxidized Low-Density Lipoprotein-Induced Angiogenesis, *Mol. Pharmacol.*, 2018, **93**, 368–375.
38 Z. Guo, K. Guan, M. Bao, B. He and J. Lu, LINC-PINT plays an anti-tumor role in nasopharyngeal carcinoma by binding to

 © 2025 The Author(s). Published by the Royal Society of Chemistry

Open Access Article. Published on 29 September 2025. Downloaded on 4/1/2026 5:04:42 PM.
This article is licensed under a Creative Commons Attribution-NonCommercial 3.0 Unported Licence.

XRCC6 and affecting its function, *Pathol. Res. Pract.*, 2024, **260**, 155460.

39 Z. Fan, Y. Liu, Y. Ye and Y. J. A. Liao, Functional probes for the diagnosis and treatment of infectious diseases, *Aggregate*, 2024, **5**, e620.

40 Y. Wang, Y. Shen, J. Li, T. Wang, J. Peng and X. Shang, Enhanced RNA secondary structure prediction through integrative deep learning and structural context analysis, *Nucleic Acids Res.*, 2025, **53**, gkaf533.

41 Z. Liu, L. Si, S. Shi, J. Li, J. Zhu, W. H. Lee, S. L. Lo, X. Yan, B. Chen, F. Fu, Y. Zheng and G. Wang, Classification of Three Anesthesia Stages Based on Near-Infrared Spectroscopy Signals, *IEEE J. Biomed. Health Inform*, 2024, **28**, 5270–5279.

42 Y. Liu, X. Li, Y. Zhang, L. Ge, Y. Guan and Z. Zhang, Ultra-Large Scale Stitchless AFM: Advancing Nanoscale Characterization and Manipulation with Zero Stitching Error and High Throughput, *Small*, 2024, **20**, e2303838.

43 H. Li, Z. Wang, Z. Guan, J. Miao, W. Li, P. Yu and C. Molina Jimenez, UCFNNet: Ulcerative colitis evaluation based on fine-grained lesion learner and noise suppression gating, *Comput. Meth. Programs Biomed.*, 2024, **247**, 108080.

44 K. Wang, S. Ning, S. Zhang, M. Jiang, Y. Huang, H. Pei, M. Li and F. Tan, Extracellular matrix stiffness regulates colorectal cancer progression *via* HSF4, *J. Exp. Clin. Cancer Res.*, 2025, **44**, 30.

45 G. Zhang, C. Song, M. Yin, L. Liu, Y. Zhang, Y. Li, J. Zhang, M. Guo and C. Li, TRAPT: a multi-stage fused deep learning framework for predicting transcriptional regulators based on large-scale epigenomic data, *Nat. Commun.*, 2025, **16**, 3611.

46 Y. Zhou, L. Li, Z. Yu, X. Gu, R. Pan, Q. Li, C. Yuan, F. Cai, Y. Zhu and Y. Cui, Dermatophagoides pteronyssinus allergen Der p 22: Cloning, expression, IgE-binding in asthmatic children, and immunogenicity, *Pediatr. Allergy Immunol.*, 2022, **33**, e13835.

47 M. Li, T. Jia, H. Wang, B. Ma, H. Lu, S. Lin, D. Cai and D. Chen, AO-DETR: Anti-Overlapping DETR for X-Ray Prohibited Items Detection, *IEEE Trans. Neural Netw. Learn. Syst.*, 2025, **36**, 12076–12090.

48 Y. Li, S. Wang, Y. Chen, M. Li, X. Dong, H. C. Hang and T. Peng, Site-specific chemical fatty-acylation for gain-of-function analysis of protein S-palmitoylation in live cells, *Chem. Commun.*, 2020, **56**, 13880–13883.

49 X. Xu, Q. Luo, J. Wang, Y. Song, H. Ye, X. Zhang, Y. He, M. Sun, R. Zhang and G. Shi, Large-field objective lens for multi-wavelength microscopy at mesoscale and submicron resolution, *Opt. Electron. Adv.*, 2024, **7**, 230212.

50 C. Zhang, Y. Dong, P. Hu, H. Fu, H. Yang, R. Yang, Y. Dong, L. Zou and J. Tan, Large-range displacement measurement in narrow space scenarios: fiber microprobe sensor with subnanometer accuracy, *Photonics Res.*, 2024, **12**, 1877–1889.